Journal Pre-proofs

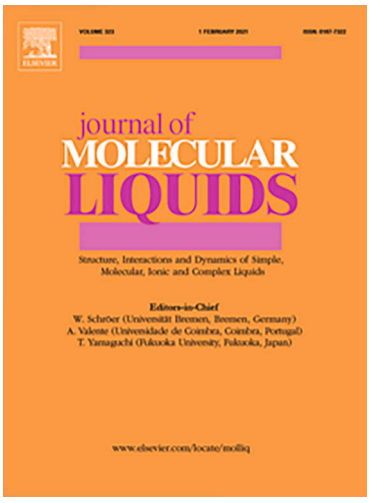

Density and viscosity of alkylammonium ionic liquids: Experimental and COSMO-RS

Murilo L. Alcantara, Gabriel L. Bressan, Paulo V.A. Santos, Maria F.V. Nobre, João A.P. Coutinho, Cláudio A.O. Nascimento, Luis A. Follegatti-Romero

PII: S0167-7322(24)02677-1
DOI: https://doi.org/10.1016/j.molliq.2024.126616
Reference: MOLLIQ 126616

To appear in: *Journal of Molecular Liquids*

Received Date: 22 August 2024
Revised Date: 19 November 2024
Accepted Date: 26 November 2024

Please cite this article as: M.L. Alcantara, G.L. Bressan, P.V.A. Santos, M.F.V. Nobre, J.A.P. Coutinho, C.A.O. Nascimento, L.A. Follegatti-Romero, Density and viscosity of alkylammonium ionic liquids: Experimental and COSMO-RS, *Journal of Molecular Liquids* (2024), doi: https://doi.org/10.1016/j.molliq.2024.126616

Density and viscosity of alkylammonium ionic liquids: Experimental and COSMO-RS

Murilo L. Alcantara[1,2]; Gabriel L Bressan[1]; Paulo V. A. Santos [1]; Maria F. V. Nobre[1]; João A. P. Coutinho[2], Cláudio A. O. Nascimento[1], Luis A. Follegatti-Romero[1]*.

[1]*Chemical Engineering Department, Polytechnic School, University of São Paulo. São Paulo-Brazil.*

[2]*CICECO - Aveiro Institute of Materials, Chemistry Department, University of Aveiro, Aveiro, Portugal*

follegatti@usp.br

ABSTRACT

The transition of our industry towards a more sustainable path requires the application of different approaches or materials. The knowledge of fluids' thermophysical properties is crucial for the analysis and assessment of innovative technologies. This study provides reliable experimental viscosities and densities of four promising alkylammonium ionic liquids (ILs): 2-hydroxyethyl ammonium ([HEA][Oc]), bis-2-hydroxyethyl ammonium ([BHEA][Oc]), tris-2-hydroxyethyl ammonium ([THEA][Oc]), and triethyl ammonium ([TEA][Oc]). These ILs were synthesized with high purity and characterized using FT-IR, Karl Fischer titration, and NMR spectroscopy. The presence of hydroxyl groups in the cations markedly increased the density and viscosity of the ILs, with a significant reduction in viscosity observed upon the removal of hydroxyl groups from [THEA][Oc]. Additionally, COSMO-RS/QSPR predictive approaches were evaluated for predicting the density and viscosity of these ILs, considering several combinations of parameterizations and ion representations. The most accurate approach presented relative deviations of 2.44% for density and 40.7% for viscosity. The use of a single experimental data at room temperature significantly lowered these deviations to 0.27% and 13.3%, respectively. This work provides valuable experimental density and viscosity data for four promising alkylammonium ILs and a predictive tool to estimate these properties for other ILs with similar structures.

Keywords: Protic ionic liquid, density, viscosity, COSMO-RS, alkylammonium.

1. Introduction

The development of innovative solvents is essential for advancing chemical processes and industrial applications. Traditional organic solvents often present environmental and health risks due to their high volatility, flammability, and toxicity In contrast, ionic liquids (ILs) have garnered significant attention from academia and industry due to their unique properties. Stable ionic interactions between large ions produce liquids with low volatility, high thermal stability, and tunability. ILs can be synthesized from a wide range of organic and inorganic ions, allowing tailored properties for diverse applications such as catalysis and separation technologies [1]. Their environmental benefits and functional versatility make ILs promising candidates for greener and more efficient industrial processes.

Ionic liquids (ILs) can be broadly classified into two main types based on the nature of their ionic bonds: aprotic ionic liquids (AILs) and protic ionic liquids (PILs). AILs lack a proton network linking the ions, which typically results in a more stable and permanent positive charge on the cation [2]. They generally exhibit lower vapor pressures compared to PILs but are often more expensive due to their complex synthesis processes and costly raw materials [3,4]. Furthermore, some AILs, particularly those based on imidazolium and fluorinated ions, can be more toxic and poorly biodegradable, which restricts their applicability in environmentally sensitive areas [2]. In contrast, PILs are characterized by a proton network connecting anions and cations, formed through proton transfer from a Brønsted acid to a Brønsted base [5]. Depending on the strength of the reagents, residual reagents may still be present within the PIL. To simplify the discussion, PILs are considered pure [6]. These mobile protons enhance ionic conductivities, which is beneficial in electrochemical applications [7]. The proton transfer reaction is typically a simple acid-base neutralization, making PIL preparation simpler and more cost-effective than AILs [8].

Alkylammonium PILs have shown promising results as solvents in various applications, including carbon capture [9], electrolysis [10], organic reactions [11], lignocellulose pretreatment [12], electrochemistry (batteries, supercapacitors, and fuel cells) [13] and liquid-liquid extraction [14]. Hydroxyl alkylammonium ILs, in particular, can enhance the solvation of insoluble natural protein polymers [15], bio-chemicals [16], and carbon dioxide [9]. However, while the presence of hydroxyl group (-OH) improves solvation capacity, it also results in increased viscosities [17].

Despite their promising properties, PILs such as alkylammonium have been less extensively explored compared to conventional AILs. This limited development is mainly attributed to their lower ionic conductivity, higher vapor pressure, and reduced thermal resistance [18]**.** However, the thermal stability of ILs synthesized from alkylamine and carboxylic acid can be enhanced by increasing the anion's alkyl chain length [19,20]. While longer alkyl chains can enhance PILs' thermal stability , they also increase viscosity and melting point temperature, which can hinder applications by reducing mass and energy transfer and causing higher pressure drops [21].

Thermophysical properties, such as density and viscosity, are crucial in determining the potential applications of these innovative ILs [22]**.** The development and simulation of new processes depend on reliable thermodynamic models, many of which, such as cubic equations of state and mass transfer models, require parameter adjustments to fit experimental density and viscosity data [23].

Thermophysical properties like density and viscosity are essential for the development of processes involving alkylammonium ILs. However, conducting high-quality experiments is often expensive and time-consuming, limiting their application to a narrow range of solute and solvent combinations [24]. This limitation underscores the need for theoretical and computational methods to complement experimental approaches.

COSMO-RS (Conductor-like Screening Model for Real Solvents) [25–27] is a quantum chemistry-based method that has gained recognition as a powerful tool for predicting thermophysical properties, such as density and viscosity, especially in systems where experimental data are scarce or

challenging to obtain. One of the main advantages of COSMO-RS is its ability to account for molecular interactions at a microscopic level, making it well-suited for the complex nature of ionic liquids (ILs) such as alkylammonium ILs. The accuracy of this model stems from its foundation in the quantum chemical description of solute-solvent interactions. These models consider the electrostatic interactions, hydrogen bonding, and van der Waals forces that are directly correlated with the macroscopic properties of ILs [28].

Machine learning-based techniques can be used to predict such properties [29]; however, they usually require high computational effort and experimental data for training. The combination of artificial intelligence (AI) with the group contribution method (GCM) was used to estimate the parameters of PC-SAFT to satisfactorily estimate liquid density, saturated vapor pressure, and critical properties [30]. Similarly, the combination of AI and COSMO can also present promising approaches to reduce the amount of data needed to train the model by using more efficient variables based on thermodynamics [31]. These models were employed to correctly predict the thermophysical properties of hexagonal boron nitride nanoparticles in deep eutectic solvents based on COSMO calculations [32]. Therefore, AI-driven corrections can utilize COSMO-RS calculations to accurately predict thermodynamic properties in cases where experimental data is lacking.

Despite their higher accuracy, these models still require high computational effort and are at early stages of development. More straightforward models may produce faster yet reliable predictions. Similar to what is performed with COSMO-RS-based models, information from COSMO sigma profiles can be used as inputs for the application of simpler predictive models, such as Quantitative Structure-Property Relationships (QSPR) [33]. COSMO-RS/QSPR-based approaches are already implemented in widely used commercial software such as ASPEN Plus [34] and COSMOtherm [35], which facilitate their application and the prediction of viscosity and density of innovative ILs. The application of COSMO-RS/QSPR models requires COSMO sigma profiles, which can be produced by applying several parameterizations and ion representations. Selecting the most suitable combination of parameterization and ion representation is crucial to producing fast and reliable predictions of densities and viscosities.

The main goal of this study is to provide experimental data on viscosity and density of promising alkylammonium-based ILs formed with octanoate anion. Furthermore, it aims to identify the combination of parameterizations and ion representations that produce the most accurate estimations of these ILs' properties via the COSMO-RS/QSPR predictive model.

2. Material and methods

2.1 Synthesis of alkylammonium PILs

All four ammonium-based PILs were synthesized using four amines and one organic acid from Sigma Aldrich with ≥99% purity. The CAS numbers and purity of the amines and acids are as follows: 2-hydroxyethylamine (141-43-5, ≥99%), bis(2-hydroxyethyl)amine (111-42-2, ≥99%), tris(2-hydroxyethyl)amine (102-71-6, ≥99%), triethylamine (121-44-8, ≥99.5%), and octanoic acid (124-07-2, ≥99%).

Four different amines were employed to generate ammonium-based cations. These include 2-hydroxyethyl amine [HEA], bis-2-hydroxyethyl amine [BHEA], and tris-2-hydroxyethyl amine [THEA], chosen to assess the impact of primary, secondary, and tertiary amines with varying ethanolamine radical counts. Additionally, triethylamine [TEA] was selected to examine the effects of omitting hydroxyl groups on IL properties. The combinations of bases and acids resulted in four PILs as shown in Table 1. The PILs were synthesized through a controlled acid-base neutralization process; more details can be found in previous studies [36,37]. Octanoic acid served as the precursor for the octanoic anion [Oc]-. Unlike most ILs derived from ethanolamine-carboxylic acid interactions, which typically yield acetate, propanoate, or butanoate-based ILs, this study leverages high-chain carboxylic acids.

Table 1. List of acids, bases, and new ammonium-based PILs synthesized in this work.

Name and structure of synthesized PILs	Abbreviation
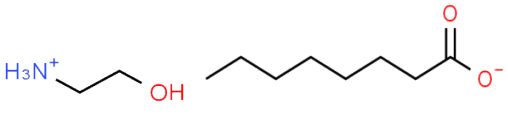 2-hydroxyethylammonium Octanoate	[HEA][Oc]
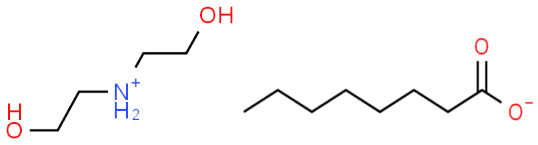 Bis-2-hydroxyethylammonium Octanoate	[BHEA][Oc]
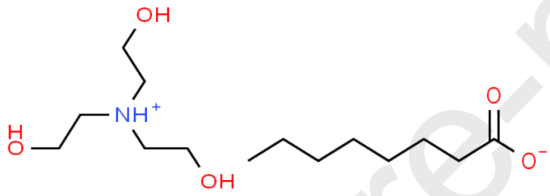 Tris-2-hydroxyethylammonium Octanoate	[THEA][Oc]
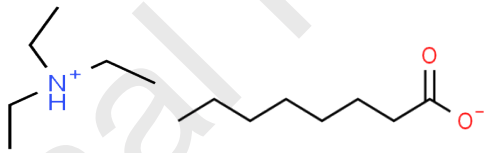 Triethylammonium Octanoate	[TEA][Oc]

One notable benefit of this IL family is their straightforward synthesis. First, the selected amine is introduced into a flask under controlled conditions, and nitrogen (99.9% purity, sourced from White Martins) is bubbled through it for 10 minutes to purge oxygen and minimize oxidation reactions. Next, pure octanoic acid is incrementally added to the amine, e, maintaining an equimolar ratio while allowing a 10 wt.% excess for the more volatile component. For all ILs except [TEA][Oc], octanoic acid was the excess component. The temperature was maintained at approximately 283.2 K using an external bath. After complete addition of reactants, the mixture was stirred for 30 minutes. The product was then placed in a rotary evaporator at 333.2 K ± 0.1K and a pressure of 0.10 ± 0.05 bar, for 24 hours to remove excess unreacted reagents, completing the IL synthesis. Further details of this synthesis method are documented in [38].

2.2 Characterization

2.2.1 Water content

The measurement of water content in these ionic liquids (ILs) is critical due to their high-water absorption potential [39] and the possible occurrence of unwanted IL degradation. Under moderate to high temperatures, deep eutectic solvents (DES) with structures similar to the studied alkylammonium ILs can convert into esters and water [40]. The acid-base neutralization reaction used in the IL synthesis is highly exothermic, potentially causing localized hot spots during the dropwise addition of reagents, which may promote unwanted esterification reactions, generating water and increasing overall water content. Therefore, maintaining low water content in synthesized ILs is crucial to confirm that these hydrophilic ILs did not absorb excess moisture from the environment and that significant esterification reactions were avoided. Water content was measured using a Metrohm 831 Karl Fischer coulometer. Methanol and Titrant 5, both sourced from Sigma-Aldrich, were used as the solvent and titrant, respectively. Water content was determined for three samples of each IL.

2.2.2 Vibrational spectroscopy

Infrared spectrophotometry was performed using Fourier-transform infrared spectroscopy (FTIR) with a Shimadzu IRPrestige-21 FTIR. The samples were inserted between two NaCl tablets. The wavelengths investigated ranged between 400 cm^{-1} and 4000 cm^{-1}. The final spectrum presented was obtained from an average of 32 scans.

Infrared absorption bands were estimated using the second derivatives of the ILs' total energies, which led to the determination of the molecular Hessian. This Hessian is crucial for predicting vibrational frequencies and generating infrared spectra within the harmonic approximation. The FINE parametrization, coupled with the ion-pair approach [41], was employed to predict the ILs' vibration frequencies and assist in the assignment of absorption bands.

2.2.3 Nuclear Magnetic Resonance Spectroscopy (NMR)

The NMR spectra were recorded at 298 K on a Magritek Spinsolve operating at 1.5 T and 60 MHz, using D_2O or methanol as the solvent. The acquisition parameters were as follows: 16384 and 1024 scans (NS), 4096 data points (TD), acquisition times (AQs) of 6.4 s and 1.6 s, repetition times of 15 s and 5 s, pulse angles of 90 and 45 degrees, and relaxation delays (d1s) of 37.43 and 20 s for ^{1}H and ^{13}C, respectively. The spectral data were processed using MestReNova software and compared with ChemDraw's estimations. All ^{1}H NMR chemical shifts are reported in δ (ppm) relative to the solvent signal (at δ 4.79 for D_2O and methanol) as an internal reference.

IL purity was measured by ^{1}H NMR area comparison of IL peaks and impurities. This approach has been applied in previous studies [18,43,44] to quantify alkylammonium-based ILs and does not account for either water or inorganic contamination. Water content was measured by Karl Fischer, and inorganic contamination was not considered due to the high purity of the reagents.

2.3 COSMO-RS/QSPR

The COSMO-RS model [25–27] is a thermodynamic predictive tool that correlates the surface charge density distributions (*σ*-profiles or sigma profiles) with their intermolecular interactions and properties of molecules. This model provides an effective and reliable approach for predicting interactions in systems containing ILs [42]. Although originally developed for broader application, COSMO-RS can provide inputs for Quantitative-Structure-Property-Relationships, which enable the prediction of thermophysical properties such as viscosity and density [33].

The sigma profiles used in this work were generated from the structural and electronic optimization of molecules via the software package TURBOMOLE [43], through its interface TMoleX v.4.5 [41].

Two parametrizations were considered in this study, both based on density functional theory (DFT) with the BP86 functional. In the first approach, the triple zeta valence polarization with diffuse functions (def2-TZVPD) basis set [41] was applied with molecular surface cavities constructed using the "FINE" approach (fine grid marching tetrahedron cavity [41]). This approach creates a COSMO surface whose segments are more uniform and evenly distributed compared to the standard COSMO cavity. The second approach considered was the universal parameter set and configuration of this "FINE" approach corresponds to that of the "BP-TZVPD-FINE_21" parametrization of COSMO-RS, available in the software package COSMOTherm v.21 [35]. This parametrization has been reported to offer advantages over classical COSMO-RS parametrizations TZVP or DMOL^3, such as improvements in the hydrogen bonding and van der Waals dispersion term and a correction for residual dielectric charge (RDC) [44,45], which usually result in better quality predictions of phase equilibrium [33,35].

Although the FINE approach offers higher accuracy for predicting phase equilibria, most COSMO-RS/QSPR implementations within commercial software, such as COSMOTherm, use parametrizations designed for classical models, such as TZVP. Therefore, despite their high accuracy in representing the charge density distribution of the molecule, the FINE approach may not provide as accurate predictions of thermophysical properties such as viscosity and density as the TZVP. This is why both parametrizations were considered in this study. The classical TZVP parametrization involves using the same density functional theory (DFT) with the BP86 functional, but with the triple zeta valence polarization functions (def-TZVP) basis set [41]. The parameter set used on COSMOTherm v.21 for this approach was "BP-TZVP_21".

The ions' representation is also crucial for the estimation of ILs' charge density distribution. The three most common representations are ion-pairs, electroneutral mixture, and the meta-file approach. In the ion-pair representation, the charge density of all ions is optimized together. This method provides accurate depictions of counterion interactions, which is beneficial for properties like molar volume, but is limited by the impracticality of considering all significant conformations due to the complexity of the conformational space [46].

The meta-file approach and electroneutral mixture perform structural and energetic optimization on each ion individually. While the former estimates the interactions of ions individually, the meta-file sums charge density profiles before calculating interaction energies. The electroneutral mixture provides the most flexible and accurate description for COSMO-RS calculations, better representing weak ion pairs, higher aggregations, and separated ions, often showing better agreement with experimental data. The meta-file, on the other hand, allows for efficient screening of numerous ILs without additional calculations and simplifies the conformational space [46].

Although the TZVP parametrization with the electroneutral mixture approach is recommended for applying both density and viscosity heuristic approaches of COSMO-RS, the FINE parametrization with ion-pair or meta-file approaches was also applied and compared with experimental data.

The ILs' densities as functions of temperature were estimated via Quantitative-Structure-Property-Relationships (QSPR), such as the ones presented on Equations (1-3) [33]. The first one was used for the estimation of molar volume $\tilde{V}_i$ at room temperature T_{room}, the second to estimate its variation with temperature $\tilde{V}_i(T)$, and the third to convert molar volume into density (ρ).

$$\tilde{V}_i(T_{room}) = c_{V_{COSMO}} V_i^{COSMO} + C_{M_2} M_{2_i} + C_{M_2^2} M_{2_i}^2 + C_{N_{Ring}} N_{ring} + \sum_k^{Elements} c_{A_k} A_i^k + c_0 \quad (1)$$

$$\tilde{V}_i(T) = c_1^T\left(\frac{T}{T_{room}} - 1\right)\tilde{V}_i(T_{room}) + c_2^T\left(\frac{T}{T_{room}} - 1\right)^2\tilde{V}_i(T_{room}) + \left[c_{V_{COSMO}}^T + c_{V_{C1}}^T\left(\frac{T}{T_{room}} - 1\right) + c_{V_{C2}}^T\left(\frac{T}{T_{room}} - 1\right)^2\right] V_i^{COSMO} + C_{M_2}^T M_{2_i} + C_{M_2^2}^T M_{2_i}^2 + C_{N_{Ring}}^T N_{ring} + \sum_k^{Elements} c_{A_k}^T A_i^k + c_0^T \quad (2)$$

$$\rho_i = \frac{MW_i}{\tilde{V}_i N_A} \quad (3)$$

Where V_i^{COSMO} is the COSMO-Volume, M_{2_i} is the second σ-moment of the compound, $M_{2_i}^2$ is the square of the compounds second σ-moment, N_{ring} is the number of ring atoms in the compound, which is zero in the cases of the studied ILs, $NiRing$ and A_i^k, the areas of surface in a given compound that belong to atoms of the same element type, where k is the element number. Additionally, eight regressed parameters (c_n) were used on the applied QSPR model for density.

Similar to the procedure applied in the density calculation, the viscosity at room temperature is estimated by one Equation (4), while its variation with temperature by Equation (5) [33].

$$\ln(\eta_i(T_{room})) = c_0 + c_{Area}A_i + c_M^2 M_i^2 + c_{N_{Ring}N_i}, Ring + c_{TS}T_{room}S_i \quad (4)$$

$$ln(\eta_i(T)) = ln(\eta_i(T_{room}) + \max[0,(c_{T0} + c_{T1}ln(\eta_i(T_{room}))))]\left(\frac{1}{T} - \frac{1}{T_{room}}\right) \quad (5)$$

The pure compound entropy S_i is computed from the difference of the total enthalpy of mixture of the pure compound and the chemical potential of the pure compound, both estimated by COSMO-RS. The two parameters c_{T0} and c_{T1} are the shift and slope of the correlation of the room temperature viscosity predictions from Equation 4 with the activation temperature of the Arrhenius-Andrade equation. Thus, temperature-dependent viscosity can be estimated by this QSPR model given seven pre-adjusted parameters. Since this model was developed for neutral organic liquids only, high deviations may be expected for ionic species, such as those studied in this paper.

2.4 Density

Experimental densities for pure and aqueous solutions of all PILs were measured using an Anton Paar DMA 4200 M densimeter, with a repeatability (precision) of 0.05 kg/m³ (0.00005 g/cm³). Measurements were taken in triplicate over a temperature range of 313.15 K to 363.15 K, except for [HEA][Oc]. The heating rate was 5 K/min, and stabilization time was 15 minutes. The densimeter employs the Pulsed Excitation Method (PEM), which utilizes a bent tube filled with the liquid sample. The tube is induced to resonant oscillation by an applied force, and the liquid's mass alters the system's resonance frequency. This frequency shift directly correlates to the liquid's density, as the tube volume remains constant. The equipment includes a temperature controller with an accuracy of 0.03 K and precision of 0.01 K. Three measurements were taken for each ILs.

Combined standard uncertainties (u_c) for densities of pure ILs were calculated according to the Guide to the Expression of Uncertainty in Measurement (GUM) [47] and Eurachem [48]. The equations for evaluating the combined standard uncertainty of densities are provided by Follegatti-Romero et al. [49]. The combined uncertainties were calculated using the following equations [50]:

$$u_c(\rho_i) = \rho_i \cdot \sqrt{\left(\frac{u_{P_i}}{P_i}\right)^2 + \left(\frac{u_{\overline{n}_j}}{n_i}\right)^2 + \left(\frac{u_{n_r}}{n_i}\right)^2} \quad (6)$$

$$u_{P_i} = 0.2\left(\frac{1-P_i}{\sqrt{3}}\right) \quad (7)$$

$$u_{\overline{n}_j} = \sqrt{\frac{\frac{1}{j-1}\sum_{j=1}^{j}(n_j-\overline{n})^2}{j}} \quad (8)$$

$$u_{n_r} = \frac{0.00002}{\sqrt{3}} \quad (9)$$

where $u_c(\rho_i)$, u_{P_i}, $u_{\overline{n}_j}$ and u_{n_r} are the combined standard uncertainty of density measurements of the compounds *i*, the uncertainty purity of compound *i*, the uncertainty from experimental measurements (*j* is the result of the *j*th measurement) and the calibration uncertainty of the densimeter utilized, respectively.

2.5 Viscosity

The viscosities of ILs were measured using an Anton Paar MCR 102 (Modular Compact Rheometer) with a repeatability (precision) of 0.05 mPa·s. The rheometer operates with a double-gap system. Approximately 0.5 mL of the IL sample was placed on the lower base, and the cone geometry was lowered to the truncation gap, allowing the system to equilibrate for 2 minutes. The lower plate's temperature was maintained at 25 °C using a P-PTD 200/AIR Peltier temperature control device. Measurements were taken at temperatures ranging from 298.15 K to 363.15 K and shear rates from 10 to 300 s^{-1}. Ten measurements were taken every 5 K with a tolerance of ±0.1 K and a stabilization time of 60 seconds. The shear rate increased linearly between measurements. The viscosity uncertainties were estimated using the same methodology employed for determining density uncertainties.

The overall uncertainty for similar procedures and equipment was previously reported to be ±0.25% of the viscosity data [51], and the same uncertainty was considered in the present study. For [HEA][Oc], measurements started at 333.1 K to prevent solidification. A temperature ramp of 1 K/min was applied, and each temperature was stabilized for 15 minutes before measurement.

After measuring the IL viscosities, the data were fitted using the Vogel-Tammann-Fulcher equation (10) [52]. The solver tool, implemented within Microsoft Excel, was used to optimize the parameters to fit the model to experimental data.

$$\eta = Ae^{B/(T-T_0)} \quad (10)$$

3. Results and discussion

3.1 IL characterization

During the neutralization reaction, the mixture of ILs and reagents produced excessive bubbles. After 24 hours of rotary evaporation, the excess unreacted solvent was removed, and a pure, yellowish, transparent viscous liquid was obtained. This liquid was characterized via FT-IR and NMR to confirm its structure and purity, while Karl Fischer titration was conducted to quantify water content.

3.1.1 Water content

The water content in alkylammonium ILs may originate from trace amounts in their reagents, particularly the hydrophilic amine component, from degradation reactions leading to amide and water formation [53,54], or from environmental moisture absorption. These ILs are known for their high selectivity for water [39] and susceptibility to evaporation. Although counterintuitive, some ILs possess non-negligible vapor pressures and can even be distilled under vacuum at moderate temperatures [55]. Consequently, alkanolammonium ILs require meticulous control during synthesis, storage, and purification to minimize water absorption, though complete elimination remains challenging.

Table 2 presents the mass percentage of water in each IL under study. All studied alkylammonium ILs showed water concentrations below 0.67 wt.%, except for [THEA][Oc], which contained approximately 1.5 wt.%. These values are relatively low compared to other studies on alkylammonium-based ILs [56–59], and the ILs were thus deemed sufficiently free of water for the purposes of density and viscosity measurement.

Table 2. The water content of four ILs

Sample	[HEA][Oc] (% g/g)	[BHEA][Oc] (% g/g)	[THEA][Oc] (% g/g)	[TEA][Oc] (% g/g)
1	0.38	0.68	1.55	0.88
2	0.40	0.70	1.53	0.63
3	0.35	0.64	1.42	0.35
Average ± std	0.38 ± 0.3	0.67 ± 0.03	1.50 ± 0.07	0.6 ± 0.3

3.1.1 Fourier-transform infrared spectroscopy (FT-IR)

Figure 1 shows the Fourier-transform infrared spectroscopy (FT-IR) analyses of the four alkylammonium ILs under study. All spectra presented similar band profiles due to the materials' similar structures and several overlapping bands between 400 cm^{-1} and 1800 cm^{-1}, making peak assignment challenging. By comparison with literature assignments [17,57,60] and absorption bands estimated by the FINE approach, the main characteristic bands were identified.

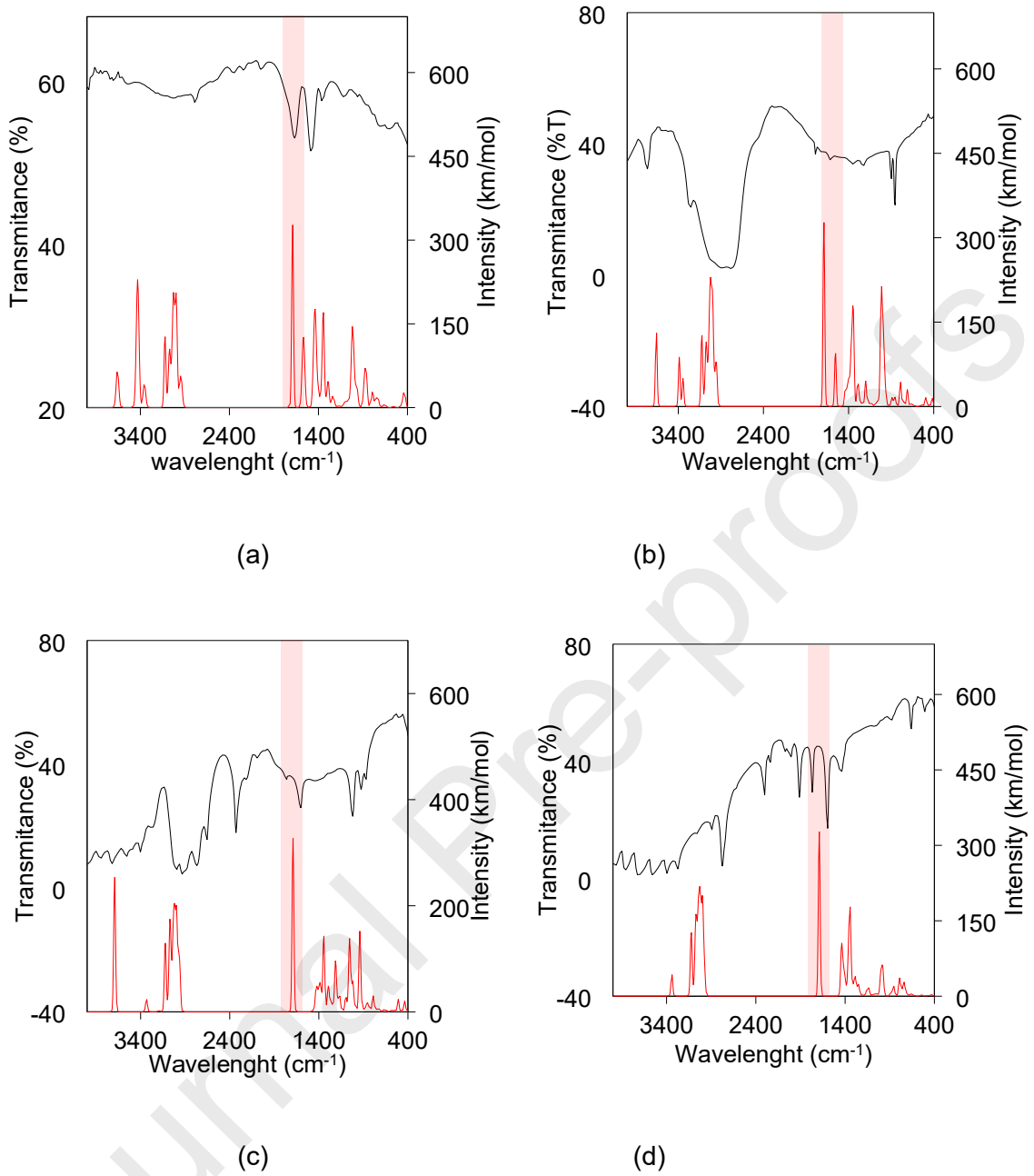

Figure 1. Comparison of experimental (black lines) and theoretical (red lines) absorption bands of (a) [HEA][Oc], (b) [BHEA][Oc], (c) [THEA][Oc], and (d) [TEA][Oc].

The ~3600 cm^{-1} absorption band was attributed to -OH stretching, primarily from cations' hydroxyls, and to a lesser extent, it could also be associated with traces of water and unreacted carboxylic acid in equilibrium with the IL, especially for [TEA][Oc]. The FINE approach predicted an increase in the intensity of this peak corresponding to the increase in cations' hydroxyl content, following the trend: [THEA] > [BHEA] > [HEA].

Peaks within the range of 2400 cm^{-1} and 3000 cm^{-1} were associated with -CH_n vibrations. The FINE approach supports this assignment; however, the predicted peaks were consistently shifted to higher wavelengths in all studied ILs. The characteristic C=O stretch vibrations of carbonyl groups

were distinctly observed at around 1700 cm^{-1}, especially for the tertiary ammonium ILs [THEA][Oc] and [TEA][Oc]. These bands were shifted to lower wavelengths in the primary [HEA][Oc] and secondary [BHEA][Oc] ammonium ILs. A range of overlapping bands from 400 to 1800 cm^{-1} is hypothesized to be related to N-H and N-C bending, wagging, and stretching vibrations, as well as C-O stretching.

3.1.2 Nuclear Magnetic Resonance Spectroscopy (NMR)

Nuclear Magnetic Resonance (NMR) spectroscopy was used to verify the ionic liquid (IL) structures indicated by FT-IR analyses. Figures 2 and 3 display the ^{1}H and ^{13}C NMR spectra for [BHEA][Oc] at 300 Hz NMR equipment, the structures of the other ILs were characterized on a 60 Hz equipment whose data and analyses can be found on the supplementary material.

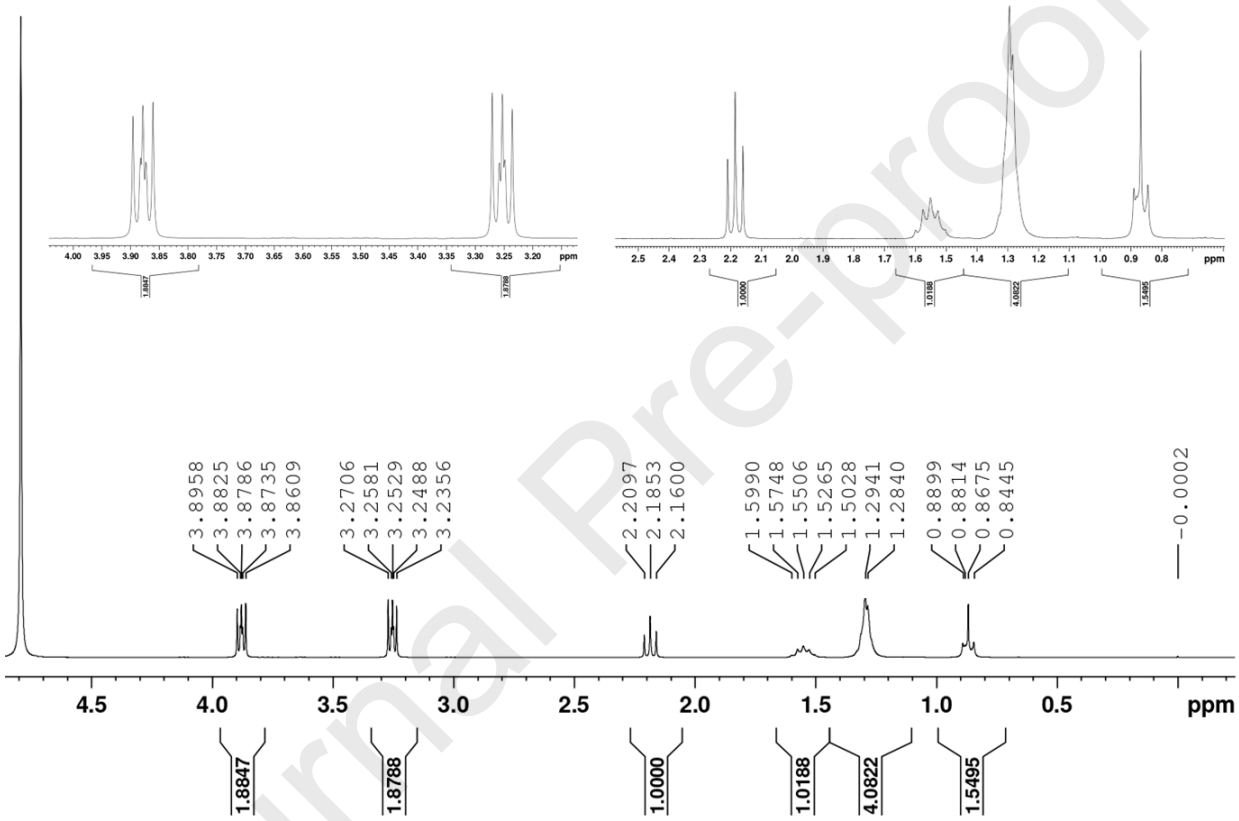

Figure 2. ^{1}H NMR of [BHEA][Oc] acquired on 300 MHz equipment using D_2O as solvent.

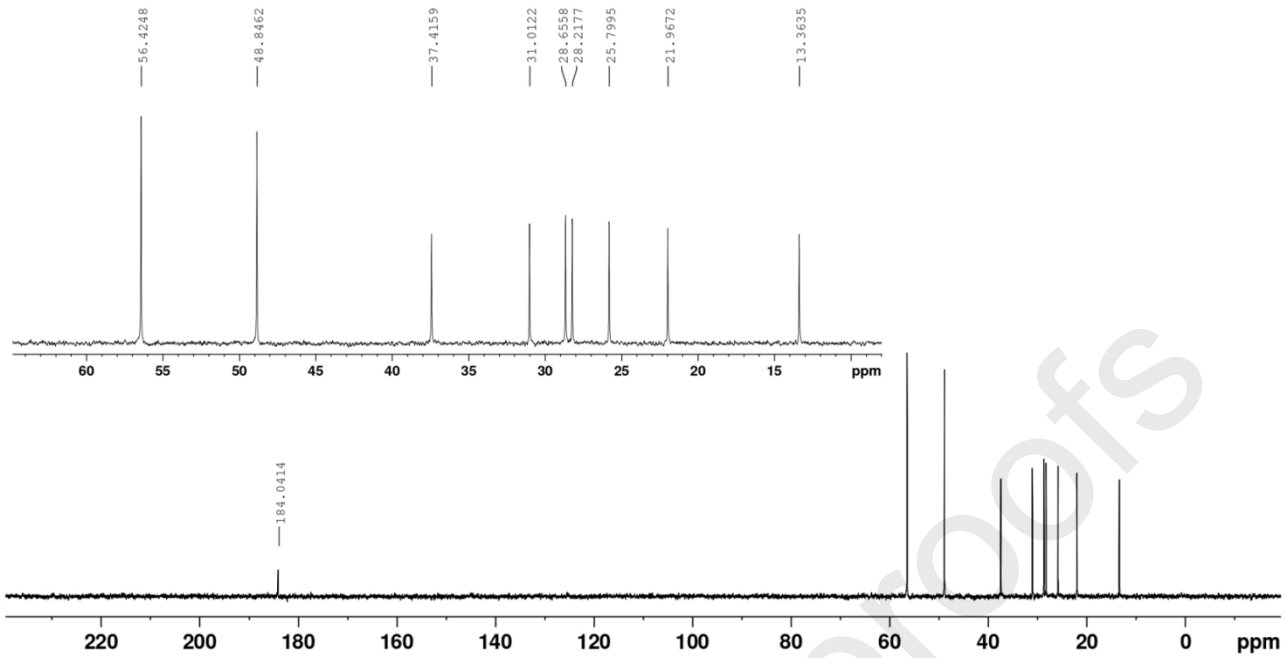

Figure 3. ^{13}C NMR of [BHEA][Oc] acquired on 300 MHz equipment using D_2O as solvent.

Table 3 outlines the identification of all signals for [BHEA][Oc]. In the ^{1}H NMR spectrum, two triplet signals at δ 3.26 and δ 3.91 were attributed to the methylene hydrogens H-9 and H-10, respectively**.** Vibrations corresponding to seven hydrogens of the octanoate anion were observed at δ 2.21, δ 1.56, δ 1.32, and δ 0.89.

Eight signals were attributed to the octanoate anion, and two to the alkylammonium cation. In the ^{13}C NMR spectrum, the signal at δ 182.67 was ascribed to the carbonyl carbon (C1). Six methylene (CH_2) signals were identified at δ 37.44, δ 26.07, δ 28.88, δ 29.3, δ 31.63, and δ 22.43, corresponding to the C2-C7 carbons. The signal for the methyl group ($-CH_3$, C8) was observed at δ 13.72. Two signals were attributed to the IL's cation at δ 48.97 and δ 56.55, corresponding to methylene groups ($-CH_2-$). The NMR spectra of [HEA][Oc], [THEA][Oc], and [TEA][Oc] exhibited similar patterns. Their respective NMR images and assignments are provided in the supplementary material (S4).

Since no peaks corresponding to organic impurities were observed in any NMR analyses of the studied ILs (Figure 2, Figure 3, and Supplementary Material S4), impurities were considered to be below twice the equipment's detection limit (0.75%). Therefore, all ILs exhibited purities above 98.5%. The absence of impurities in ^{1}H NMR spectra was previously reported by our group [61]**.** However, such results are not commonly observed for alkylammonium ILs [17,37,62].

Table 3. ^{1}H and ^{13}C NMR of [BHEA][Oc]

Structure	Position	^{1}H NMR signals	^{13}C NMR signals
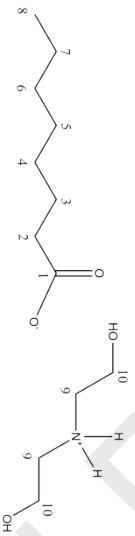	1	-	182.67
	2	2.21	37.44
	3	1.56	26.07
	4	1.32	28.88
	5	1.32	29.3
	6	1.32	31.63
	7	1.32	22.43
	8	0.89	13.72
	9	3.26	48.97
	10	3.91	56.55

3.2 COSMO-RS/QSPR

The charge density distribution of the alkylammonium ILs under study is depicted in Figures 6 and 7, according to the separated ions and ion-pair representations, respectively. The reddish areas represent highly electronegative sites of the molecule (hydrogen acceptors), the bluish areas indicate positively charged sites of the molecule (hydrogen donors), and the green areas correspond to predominant electroneutral sites. The triethylammonium cation $[TEA]^{+}$ (Figure 4 (a)) displays a more homogeneous charge dispersion. In contrast, the ethanolamine-based cations $[HEA]^{+}$, $[BHEA]^{+}$, and $[THEA]^{+}$ (Figure 4 (b) to (d)) predominantly show bluish areas near the ammonium radicals and hydrogens of the hydroxyl groups, along with reddish areas associated with the oxygens of the hydroxyls. The octanoic anion [Oc]- (Figure 4 (e)) displays a prominent red area linked to the carboxyl group and an extensive green area corresponding to the hydrocarbon chain.

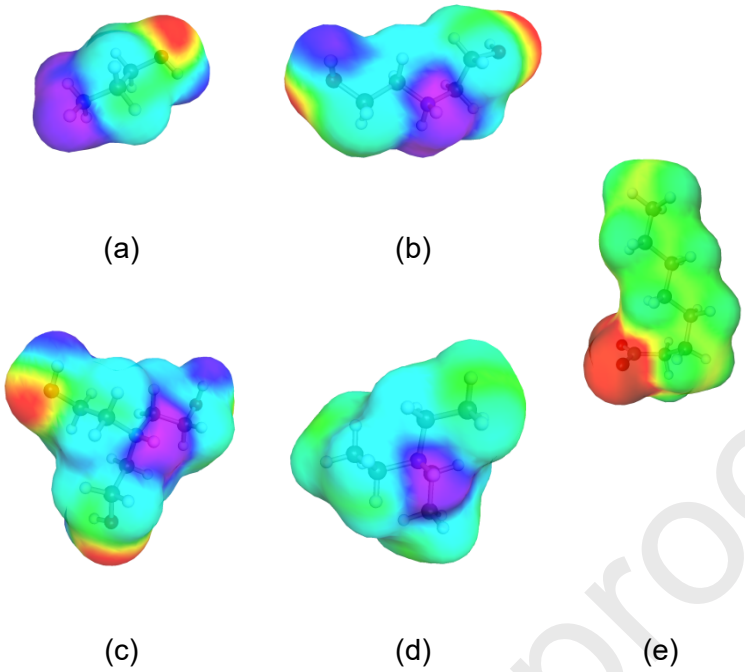

Figure 4. Visualization of charge density distribution of separated ions: (a) 2-Hydroxyethylammonium $[HEA]^+$, (b) bis(2-Hydroxyethyl)ammonium $[BHEA]^+$, (c) Tri-(2-Hydroxyethyl)ammonium $[THEA]^+$, (d) Triethylammonium $[TEA]^+$, (e) Octanoate $[Oc]^-$.

By comparing the images of separated ions (Figure 4) and ion-pairs (Figure 5), it is possible to observe that the ion-pair representation displays significantly fewer reddish and bluish spots, indicating a reduced concentration of highly charged sites. A more precise evaluation of their charge distributions can be found in the supplementary material. The lower concentration of highly charged spots in the ion-pair suggests that this approach should result in weaker intermolecular interactions, thereby producing ILs with lower densities and viscosities.

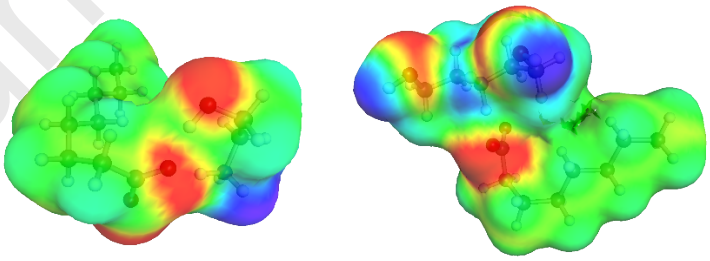

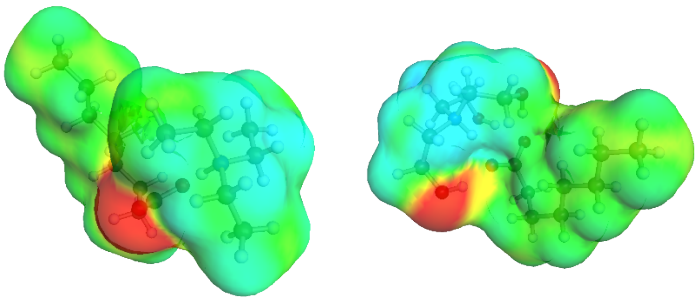

(c) (d)

Figure 5. Visualization of charge density distribution and structures of ion-pairs under study: (a) 2-Hydroxyethylammonium Octanoate [HEA][Oc], (b) bis(2-Hydroxyethyl)ammonium Octanoate [BHEA][Oc], (c) Tri-(2-Hydroxyethyl)ammonium Octanoate [THEA][Oc], (d) Triethylammonium Octanoate [TEA][Oc].

3.3 Comparison of models

Figure 6 presents graphs comparing five approaches for estimating the alkylammonium ILs' densities and viscosities. COSMO-RS predictions of density provided more accurate estimations than viscosity, presumably due to the QSPR parameters of viscosity being regressed only for neutral organic liquids [33]. The COSMO-RS predicted data follow the same trend as the experimental data, as indicated by its nearly constant distance to the diagonal.

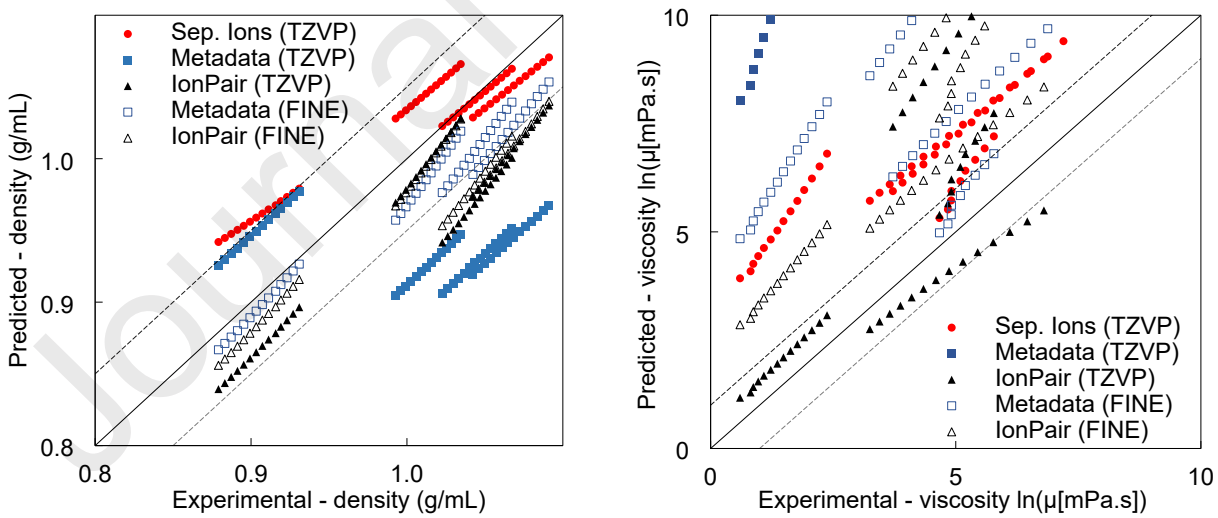

(a) (b)

Figure 6. Comparison of experimental and COSMO-RS prediction of (a) densities and (b) viscosities, considering five different representations and the data of all four ILs under study.

Table 4 presents the average absolute and relative deviations of the five approaches evaluated. Although the FINE parametrization better describes the ions' charge distribution and is reported to promote more accurate phase equilibrium predictions, the TZVP parametrization presented the overall lowest deviations, except for the metadata approach. This is presumably due to the QSPR/COSMO-RS parameters being regressed to density and viscosity data using TZVP parametrization. A fair comparison would require a QSPR model with parameters regressed considering the FINE parametrization.

Table 4. Absolute and relative average deviations of COSMO-RS density and viscosity given 5 IL representations.

Approaches	Density		Viscosity	
	AAD (g/mL)	ARD (%)	AAD ln(μ[mPa.s])	ARD[a] (%)
Metadata (TZVP)	0.093	9.58	16.3	455
Separated ions (TZVP)	0.027	2.96	2.34	102
Ion-pair (TZVP)	0.047	4.89	1.84	44.5
Metadata (FINE)	0.03	3.01	3.58	144
Ion-pair (FINE)	0.039	4.03	3.29	102

[a]Relative deviation of ln(μ)

Table 5 allows for the comparison of models according to each IL. It is possible to observe that the separated ions (TZVP) approach produced the lowest deviations in density and viscosity for [HEA][Oc], [BHEA][Oc], and [THEA][Oc], while the ion-pair (TZVP) approach showed the lowest deviations for [TEA][Oc]. These evaluations confirm that TZVP parametrization is the most suitable for the prediction of thermophysical properties of alkylammonium ILs via COSMO-RS/QSPR approach.

Since the primary difference among these ILs is the presence of hydroxyl groups, additional recommendations can be made regarding the structural representation of ILs in the COSMO-RS/QSPR predictive approach. In the absence of further data, the separated ions representation is recommended for predicting the thermophysical properties of hydroxyalkylammonium ILs, while the ion-pair approach is advised for hydroxyl-free alkylammonium ILs. Following this recommendation, the ARD of COSMO-RS/QSPR predictions is 2.44% for density and 40.7% for viscosity.

Table 5. Absolute and relative average deviations of COSMO-RS density and viscosity of ILs under study.

ILs	Metadata (TZVP)	Separated ions (TZVP)	Ion-pair (TZVP)	Metadata (FINE)	Ion-pair (FINE)
ARD of Density					
[HEA][Oc]	9.1%	3.4%	1.6%	2.7%	1.7%
[BHEA][Oc]	11.7%	0.3%	7.5%	3.8%	6.1%
[THEA][Oc]	12.1%	1.7%	6.1%	4.5%	5.9%
[TEA][Oc]	5.4%	6.5%	4.4%	1.1%	2.3%
ARD of Viscosity					
[HEA][Oc]	279%	20%	26%	13%	71%
[BHEA][Oc]	373%	43%	88%	54%	102%
[THEA][Oc]	469%	51%	16%	129%	39%
[TEA][Oc]	700%	293%	48%	378%	195%

From Figure 6, it is evident that the distance between the predicted and experimental data points is nearly constant across all temperatures for a given IL and parametrization. This consistency suggests that the QSPR/COSMO-RS model accurately predicts the temperature dependence of thermophysical properties (Equations 2 and 5). However, the model exhibits a systematic deviation when estimating room temperature properties (Equations 1 and 4), leading to a nearly uniform offset between predictions and experimental values.

To address this limitation, a correction was applied by adding a constant value to the COSMO-RS predicted properties. This constant corresponds to the difference between the experimental and predicted values at room temperature. Figure 7 presents a comparison between this corrected approach and the experimental data. Comparing Figure 7 with Figure 6, it is evident that correcting a single experimental thermophysical property at room temperature significantly increased the model's

accuracy, especially for density, where deviations were found to be below ±0.02 g/mL regardless of the model or IL.

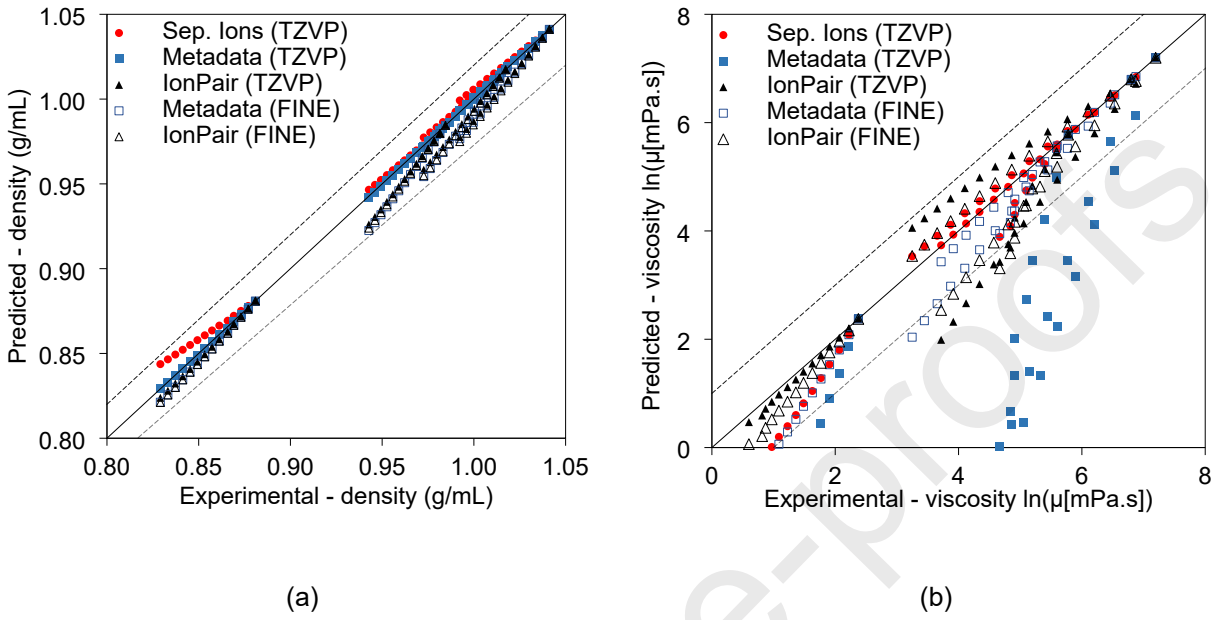

(a) (b)

Figure 7. Experimental and COSMO-RS prediction of (a) densities and (b) viscosities, corrected with room temperature thermophysical data.

The model comparison shown in Table 6 confirms that after room temperature correction, the TZVP parametrization still produces the most accurate estimations of viscosity and density for alkylammonium ILs. The separated ions approach remains recommended for alkylammonium PILs containing hydroxyl groups on the cation, while the ion-pair approach provides more accurate results for hydroxyl-free alkylammonium PILs. The application of the room temperature correction reduced the ARD from 2.44% to 0.27% for density, and from 40.7% to 13.3% for viscosity.

Table 6. Relative average deviations of QSPR/COSMO-RS prediction of density and viscosity of ILs under study, considering the correction of room temperature property.

ILs	Metadata (TZVP)	Separated Ions (TZVP)	IonPair (TZVP)	Metadata (FINE)	IonPair (FINE)
			ARD of Density		
[HEA][Oc]	0.05%	0.17%	0.90%	1.11%	1.02%
[BHEA][Oc]	0.03%	0.21%	0.76%	0.97%	0.95%
[THEA][Oc]	0.06%	0.33%	0.76%	0.80%	0.90%
[TEA][Oc]	0.02%	0.82%	0.38%	0.54%	0.55%
			ARD of Viscosity		
[HEA][Oc]	159%	25%	40%	22%	44%
[BHEA][Oc]	425%	1.0%	87%	10%	58%
[THEA][Oc]	462%	16%	50%	57%	22%
[TEA][Oc]	237%	78%	11%	89%	36%

3.4 Density

Experimental density data obtained at 0.1 MPa are summarized in Table 7. As noted in the footnote of Table 7, the combined standard uncertainty for the density of [HEA][Oc] (purity 99.62%) was 0.4 kg/m³ (relative uncertainty: 0.0004), while for [THEA][Oc] (purity 98.5%), it was 1.4 kg/m³ (relative uncertainty: 0.0018). This highlights that the primary source of density measurement uncertainty is likely the impurities present in the samples (water in this case), as also reported by Chirico et al. [63]. Further details on the calculation of uncertainties are available in the report published in the literature [63].

Table 7. Experimental density (kg/m³) of ILs from T = (298.15 to 363.15) K at 0.1 MPa

T/K	[HEA][Oc][a]	[BHEA][Oc][b]	[THEA][OC][c]	[TEA][OC][d]
298.15	880.92	1041.12	1017.31	984.51
303.15	876.99	1037.36	1013.94	981.51
308.15	873.07	1033.61	1010.52	978.31
313.15	869.15	1029.84	1007.10	975.09
318.15	865.80	1026.08	1003.69	971.89
323.15	861.24	1022.32	1000.28	968.68
328.15	857.28	1018.57	996.87	965.47
333.15	853.30	1014.81	993.46	962.27
338.15	849.31	1011.03	990.04	959.05
343.15	845.31	1007.26	986.60	955.83
348.15	841.30	1003.47	983.16	952.59
353.15	837.26	999.70	979.69	949.34
358.15	833.20	995.97	976.20	946.07
363.15	829.10	992.32	972.67	942.75

Type B evaluation of standard uncertainties u for temperature and pressure are $u(T)$=0.1 K. Combined standard uncertainties are: [a] $u_c(\rho)$=0.4 kg.m^{-3}; [b] $u_c(\rho)$=0.7 kg.m^{-3}; [c] $u_c(\rho)$=1.4 kg.m^{-3}; [d] $u_c(\rho)$=0.6 kg.m^{-3}

Figure 8 presents the COSMO-RS estimations alongside the experimental densities of the investigated ILs. The experimental results show that the presence of hydroxyl groups significantly elevates the densities of the ILs in the order of [THEA][Oc] > [BHEA][Oc] > [HEA][Oc] > [TEA][Oc]. The primary structural distinction among these ILs is the presence or absence of -OH radicals at the ends of ethyl groups. A notable discrepancy was observed between the densities of ILs containing -OH radicals ([THEA], [BHEA], and [HEA]) compared to [TEA][Oc], which lacks hydroxyl groups.

According to the recommendation of the previous section, the separated ions approach using TZVP parametrization was applied to estimate all hydroxy ammonium ILs ([HEA][Oc], [BHEA][Oc], and [THEA][Oc]), while ion-pair with FINE parametrization was utilized used for the hydroxyl-free alkylammonium [TEA][Oc]. The completely predictive approach shown in Figure 8 presents qualitative agreement with the experimental data, however, still presents much lower deviation compared to the COSMO-RS approach corrected by room temperature density. Additional data and details can be found in the supplementary material.

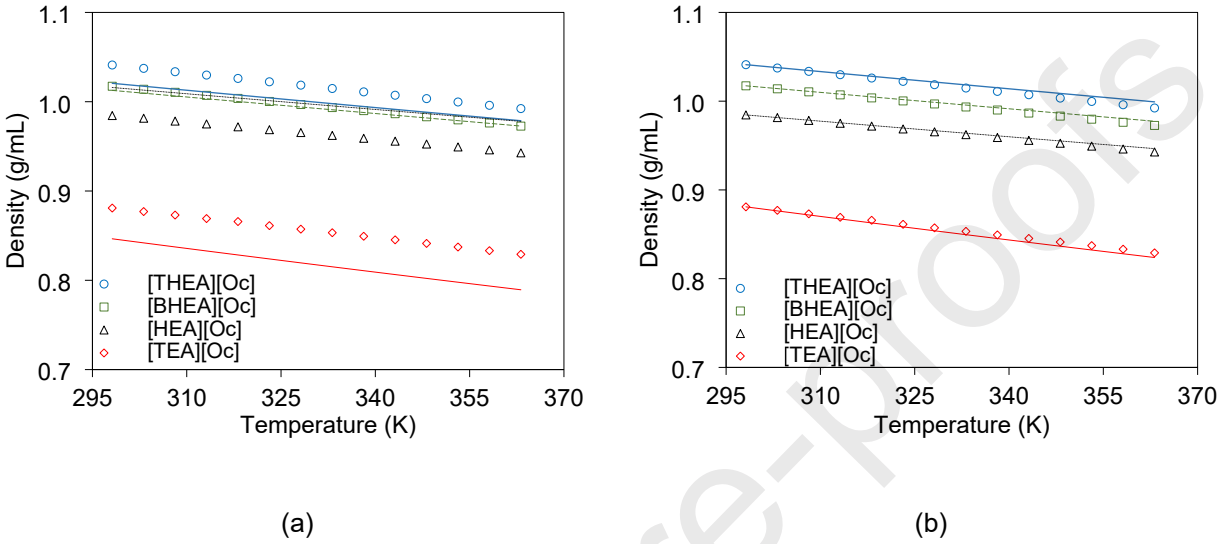

Figure 8. Experimental (dots) and COSMO-RS predicted (lines) densities of [THEA][Oc] (blue), [BHEA][Oc] (green), [HEA][Oc] (black), and [TEA][Oc] (red), (a) considering fully predicted approach, or (b) room temperature corrected approach.

3.5 Viscosity

Experimental viscosity data (μ) of synthesized ILs at different temperatures are reported in Table 8. As indicated in the footnote of Table 8, the combined standard uncertainty for the density of [HEA][Oc] (purity: 99.62%) was 0.002 mPa·s, corresponding to a relative uncertainty of 0.0004. In contrast, for [THEA][Oc] (purity: 98.5%), the combined standard uncertainty was 0.03 mPa·s, with a relative uncertainty of 0.0008. As observed, water content affects the uncertainties of pure ILs.

Table 8. Experimental viscosity (mPa·s) of ILs from *T* = (298.15 to 363.15) *K* at 0.1 MPa

T/K	[HEA][Oc]	[BHEA][Oc]	[THEA][OC]	[TEA][OC]
298.15	-	7.19668	6.79807	2.37490

303.15	-	6.87596	6.45934	2.22213
308.15	-	6.53250	6.10264	2.06610
313.15	-	6.20486	5.76531	1.90823
318.15	-	5.89437	5.44703	1.76895
323.15	5.77669	5.59975	5.14656	1.62943
328.15	5.58964	5.32086	4.86283	1.48539
333.15	5.39680	5.05662	4.59540	1.36172
338.15	5.19645	4.80467	4.34158	1.22639
343.15	5.09442	4.57180	4.10075	1.08647
348.15	4.91214	4.33990	3.87149	0.97104
353.15	4.90830	4.12199	3.65299	0.87045
358.15	4.84047	3.91456	3.44594	0.81483
363.15	4.66767	3.71734	3.24761	0.59982

Type B evaluation of standard uncertainties u for temperature and pressure are $u(T)$=0.1 K. Combined standard uncertainties are: [a] $u_c(\mu)$=0.002 mPa·s; [b] $u_c(\mu)$= 0.004 mPa·s; [c] $u_c(\mu)$=0.03 mPa·s; [d] $u_c(\rho)$= 0.002 mPa·s

Figure 9 presents the experimental and predicted viscosities of the studied ILs as functions of temperature. As expected, an increase in temperature reduced viscosity, with [HEA][Oc] exhibiting the highest viscosity among the alkylammonium ILs studied. Data for this IL were acquired at temperatures above 323 K to prevent the risk of solidification in the equipment. [BHEA][Oc] and [THEA][Oc] showed moderate decreases in viscosity with temperature, while [TEA][Oc] demonstrated significantly lower viscosities.

The presence of hydroxyl groups (-OH) plays a crucial role in controlling the viscosities of these PILs. At near-room temperature, [TEA][Oc] exhibited a viscosity of 10.75 mPa.s, while [THEA][Oc] presented a much higher viscosity of 896.1 mPa.s, an increase of nearly 90 times. Given that the only structural difference between [TEA][Oc] and [THEA][Oc] is the presence of three hydroxyl groups on the latter, it is evident that -OH groups significantly influence IL viscosity. This increase in viscosity strongly indicates hydrogen bond formation, further supported by charge density distributions (sigma

profiles) shown in Figure S3. High concentrations of peaks above 0.01 e/Å² or below -0.01 e/Å² are indicative of hydrogen bonding. While all hydroxyalkylammonium ILs exhibit peaks in the hydrogen bond range, [TEA][Oc] has most of its segments within the neutral charge range of [-0.01 e/Å², 0.01 e/Å²].

COSMO-RS/QSPR overestimated the viscosities of all alkylammonium ILs and incorrectly predicted the order of [HEA][Oc]. This deviation likely stems from the original QSPR model's lack of consideration for ionic species during parameter regression. However, when corrected for room temperature, COSMO-RS/QSPR predictions aligned more closely with experimental values (Figure 9 (b)). These results confirm that the QSPR model effectively captures viscosity variations with temperature, though it struggles with absolute room temperature viscosity predictions. While only a limited dataset was evaluated, these findings underscore the promising application of the COSMO-RS/QSPR model for predicting viscosities of other ionic liquids (ILs). This capability facilitates the consideration of alkylammonium-based solvents in screening innovative materials and conceptual process development.

Given the importance of the Vogel-Tammann-Fulcher (VTF) model for commercial software such as ASPEN and ProII, VTF model parameters were regressed to experimental viscosity data. Figure S4 demonstrates high agreement, with R² above 0.996, and Table S1 presents all regressed parameters.

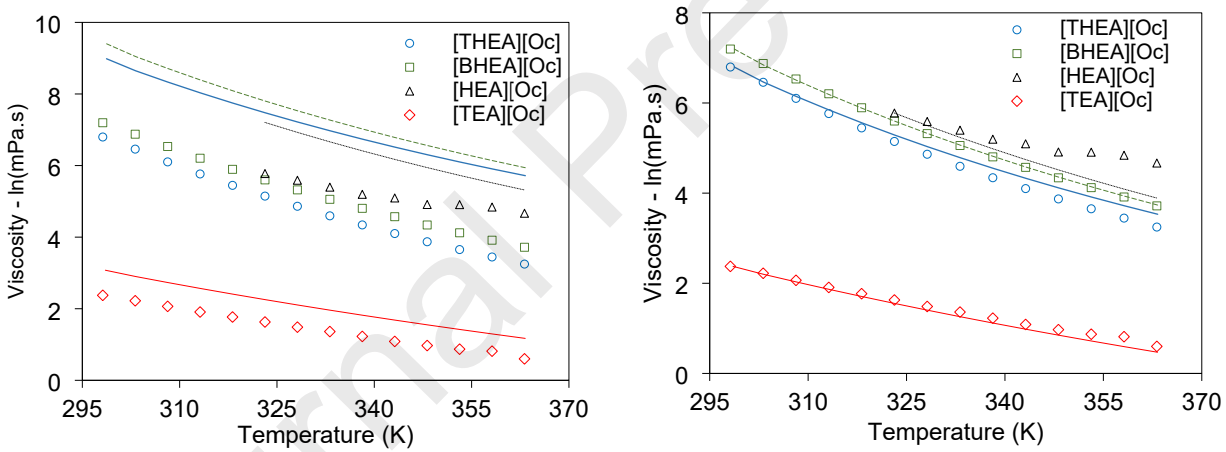

Figure 9. Experimental (dots) and COSMO-RS predicted (lines) viscosities of [THEA][Oc] (blue), [BHEA][Oc] (green), [HEA][Oc] (black), and [TEA][Oc] (red), (a) considering fully predicted approach, or (b) room temperature corrected approach.

Figure 10 illustrates a comparison of room temperature viscosities of several ILs and organic solvents. The hydroxyalkylammonium PILs exhibited significantly higher viscosities, even when compared to other ILs, with values approaching those of glycerol. In contrast, the alkylammonium IL lacking a hydroxyl group, [TEA][Oc], demonstrated much lower viscosity. [DEA][Bu], another alkylammonium IL formed from a hydroxyl-free amine and a carboxylic acid, also was reported to present room temperature viscosity close to water [17], reaffirming that alkylammonium ILs without hydroxyl groups on the cation present significantly lower viscosities compared to other ILs.

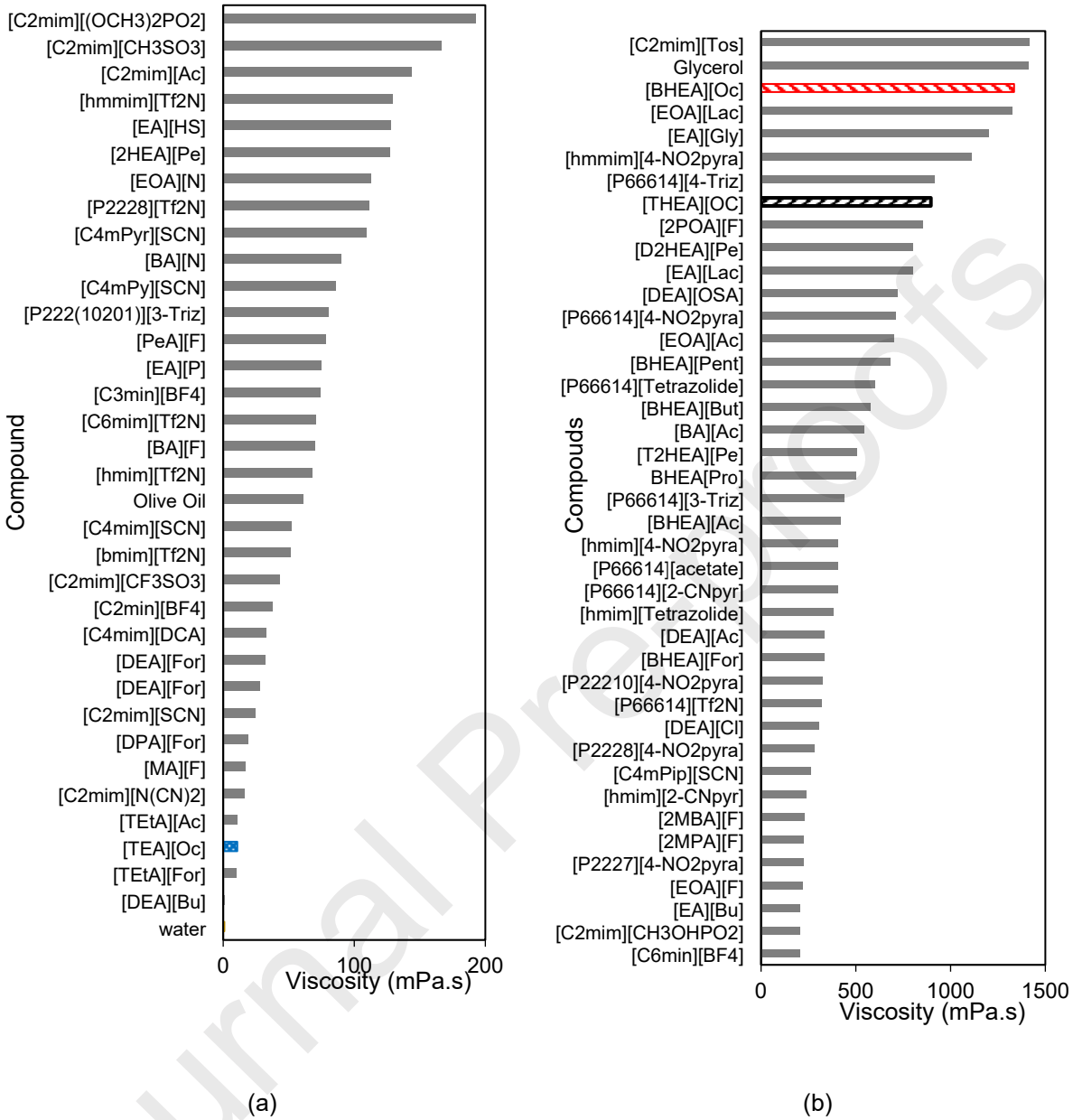

Figure 9. Comparison of ILs' viscosities at 298 K ranging from (a) 0-200 cp, and (b) 200 -1500 cp.

Alkylammonium-based ILs, particularly those without hydroxyl groups, exhibit significantly lower viscosities compared to many organic solvents and ionic liquids. This highlights their potential advantages in various technological applications. The COSMO-RS/QSPR predictive tool, when properly parameterized, provides accurate predictions of viscosities and densities for other alkylammonium derivatives, thereby accelerating the development of innovative and sustainable technologies.

4. Conclusion

Four protic ionic liquids (ILs) were synthesized using alkylammonium cations paired with octanoate anions. The synthetized ILs included three cations containing hydroxyl groups—2-hydroxyethyl ammonium octanoate ([HEA][Oc]), bis(2-hydroxyethyl)ammonium octanoate ([BHEA][Oc]), and tris(2-hydroxyethyl)ammonium octanoate ([THEA][Oc])—and one without hydroxyl groups, triethyl ammonium octanoate ([TEA][Oc]). ILs' structures were characterized by FT-IT, and NMR; the latter was also used to confirm their high purity (>98.5%). Water contents below 0.67 wt.% were obtained for all ILs, except for the [THEA][Oc], which presented 1.50 wt.%. These values were considered low if compared with other alkylammonium IL.

The experimental viscosity and density data were measured from 313.15 K to 363.15 K, with both properties exhibiting expected variations with temperature. The densities and viscosities of the studied alkylammonium ILs followed the order: [THEA][Oc] > [BHEA][Oc] > [HEA][Oc] > [TEA][Oc]. A significant difference was observed between the thermophysical properties of [TEA][Oc] and the other ILs, particularly for viscosity. For example, adding three hydroxyl groups to triethylammonium octanoate ([TEA][Oc]) dramatically increased its room temperature viscosity from 10.75 mPa.s to 896.1 mPa.s. This effect was attributed to the absence of hydroxyl groups in [TEA][Oc], which likely reduces intermolecular interactions due to hydrogen bonding. Comparisons of viscosities among various ILs indicate that hydroxyalkylammonium ILs exhibit moderate to high viscosities, whereas hydroxyl-free ILs, such as [TEA][Oc] and [DEA][Bu], display significantly lower viscosities, approaching the same order of magnitude as water.

Five COSMO-RS/QSPR approaches were evaluated for predicting the densities and viscosities of alkylammonium ILs. The classical TZVP parametrization yielded lowest deviations from experimental values , likely due to the QSPR model parameters were optimized for TZVP-parametrized molecules. The separated ions approach performed best for hydroxyalkylammonium ILs, while the ion-pair approach was most suitable for hydroxyl-free alkylammonium ILs. The fully predictive approach resulted in average relative deviations (ARD) of 2.44% for density and 40.7% for viscosity. A key source of deviation was the inaccurate estimation of room-temperature properties. However, applying a fixed correction to the COSMO-RS/QSPR predictions, deviations were substantially reduced, achieving ARDs of 0.27% for density and 13.3% for viscosity. This findings demonstrates the potential of COSMO-RS/QSPR to reliably estimate viscosities of alkylammonium ILs when a single room temperature property is known.

The experimental data and COSMO-RS/QSPR predictive approach for density and viscosity of alkylammonium ILs are expected to be of great interest for the development of innovative technologies utilizing these sustainable fluids. The study of the influence of hydroxyl groups on these ILs' thermophysical properties provides fundamental insights and guides the screening and application of these materials.

CRediT authorship contribution statement

Murilo L. Alcantara:Conceptualization, visualization, Methodology, software, Supervision, Writing – original draft, review & editing; **Gabriel L. Bressan**: Investigation, data curation, methodology, Methodology, Writing – original draft. **Paulo V. A. Santos**: data curation, methodology, Methodology, Writing – original draft; **Maria F. V. Nobre**: data curation, methodology, Methodology, Writing – original draft; **João A. P. Coutinho**: Resources, Supervision, Writing – review & editing **Luis A. F. Romero**: Project administration, Resources, Supervision, Writing – review & editing.

Supplementary Materials

S1 Extra Figures and Tables

S2 Charge density distribution

S3 Fourier-transform infrared spectroscopy (FTIR)

S4 Nuclear Magnetic Resonance Spectroscopy (NMR)

S5 Density and Viscosity

Acknowledgements

This work was developed within the scope of projects financed by the São Paulo Research Foundation (FAPESP) and CICECO Aveiro Institute of Materials. FAPESP grants' numbers are grant numbers 2021/07155-6, 2019/22085-4, and 2024/04898-6 while CICECO's projects were UIDB/50011/2020, UIDP/50011/2020 & LA/P/0006/2020, financed by national funds through the FCT/MCTES (PIDDAC). Additionally, we acknowledge the National Council for Scientific and Technological Development (CNPq) for their contribution via the PIBIC financial support program. We also appreciate the financial backing from Petronas (Petroliam Nasional Berhad) for Project No. ANP 23708-1.

Declaration of generative AI and AI-assisted technologies in the writing process

During the preparation of this work the author(s) used ChatGPT 4.0 in order to increase the readability and correct grammar and typo mistakes. After using this tool/service, the author(s) reviewed and edited the content as needed and take(s) full responsibility for the content of the publication.

NOMENCLATURE

[HMIm][F_4B]	1-hexyl-3-methylimidazolium tetrafluoroborate
[HMIm][HySp]	1-hexyl-3-methylimidazolium hydrogensulphate
[HySp]	hydrogensulphate
[F_4B]	tetrafluoroborate
[F_3Ac]	trifluoroacetate
[AMIm][($F_3MeSu)_2A$]	1-alkyl-3-methylimidazolium bis(trifluoromethanesulfonyl)amides
[BMIm][NTf_2]	1-butyl-3-methylimidazolium bis(trifluoromethanesulfonyl)amide
[BMIm][($F_3MeS)_2A$)]	1-butyl-3-methylimidazolium bis(trifluoromethanesulfonyl)amide
[BMIm][Ac]	1-butyl-3-methylimidazolium acetate
[BMIm][C]	1-*n*-butyl-3-methylimidazolium-2-carboxylate
[BMIm][Cl]	1-butyl-3-methylimidazolium chloride
[BMIm][Cl]*	1-butyl-3-methylimidazolium chloride

[BMIm][$F_3(F_5E)_3P$]	1-butyl-2,3-dimethylimidazolium trifluorotris(pentafluoroethyl) phosphate
[BMIm][F_4B]	1-butyl-3-methylimidazolium tetrafluoroborate
[BMIm][F_6P]	1-butyl-3-methylimidazolium hexafluorophosphate
[BMIm][MSu]	1-butyl-3-methylimidazolium methylsulfonate
[BMMIm][Cl]	1-butyl-2,3-dimethylimidazolium chloride
[BMMIm][Cl]*	3-butyl-1,2-dimethylimidazolium chloride
[BMMIm][F_3MeSu]	1-butyl-2,3-dimethylimidazolium trifluoromethanesulfonate
[DEA][Bu]	diethylammonium butanoate
[EMIm][F_4B]	1-ethyl-3-methylimidazolium tetrafluoroborate
[EMIm][F_3MeSu]	1-ethyl-3-methylimidazolium trifluoromethanesulfonate
[EMMIm][Ni]	1-ethyl-2,3-dimethylimidazolium nitrite
[EMMIm][Ni]	1-ethyl-2,3-dimethylimidazolium nitrite
[HMIm][F_4B]	1-hexyl-3-methylimidazolium tetrafluoroborate
$[Ru(CO)_3Cl_2]_2$	tricarbonyldichlororuthenium(II) dimer
[Xantphos]	4,5-bis(diphenylphosphine)-9,9-dimethylxanthene
AC	Activated carbon
FTS	Fisher-Tropsch synthesis
HCPs	Hypercrosslinked polymers
HCs	hydrocarbons
HIPs	Hypercrosslinked ionic polymers
IL	ionic liquids
ILSS	ionic liquid supported synthesis
Im	Imidazolium
M-NPs	metal nanoparticles
RWGS	reverse water-gas shift
SILP	supported ionic liquid phase
TOF	turnover frequency
TRL	technology readiness level

WGS	water-gas shift
RTIL	Room temperature ionic liquid
FE	Faradaic efficiency
HKUST	Hong Kong University

REFERENCES

[1] P. Tomar, D. Jain, A REVIEW OF GREEN SOLVENT IONIC LIQUIDS: AS A FUTURE SOLVENT, J Adv Sci Res 13 (2022) 1–16. https://doi.org/10.55218/JASR.202213601.

[2] A. Mirjafari, L.N. Pham, J.R. McCabe, N. Mobarrez, E.A. Salter, A. Wierzbicki, K.N. West, R.E. Sykora, J.H. Davis, Building a bridge between aprotic and protic ionic liquids, RSC Adv. 3 (2013) 337–340. https://doi.org/10.1039/C2RA22752E.

[3] A. Latała, M. Nędzi, P. Stepnowski, Toxicity of imidazolium ionic liquids towards algae. Influence of salinity variations, Green Chem. 12 (2010) 60–64. https://doi.org/10.1039/B918355H.

[4] B. Peric, Evaluation of (eco) toxicity and biodegradability of short aliphatic protic ionic liquids, (2014).

[5] T.L. Greaves, C.J. Drummond, Protic Ionic Liquids: Evolving Structure–Property Relationships and Expanding Applications, Chem Rev 115 (2015) 11379–11448. https://doi.org/10.1021/acs.chemrev.5b00158.

[6] T. Yasuda, M. Watanabe, Protic ionic liquids: Fuel cell applications, MRS Bull 38 (2013) 560–566. https://doi.org/10.1557/mrs.2013.153.

[7] A. Mota-Lima, M.L. Alcantara, F.J. Pérez-Sanz, R.C. Bazito, P. Vidinha, R.M.B. Alves, C.A. Oller Nascimento, Review—High-Pressure Carbon Dioxide Separation Using Ionic Liquids: A CO 2 -Electrocatalysis Perspective, J Electrochem Soc 168 (2021) 086502. https://doi.org/10.1149/1945-7111/ac085d.

[8] D. Santos, É. Lourenço, M.F.C. Santos, E. Franceschi, C. Dariva, A. Barison, A. Zuber, M. Castier, S. Mattedi, Volumetric properties of binary aqueous solutions of protic ionic liquids based on bis (2-hydroxyethyl) ammonium, J Mol Liq 222 (2016) 867–872. https://doi.org/10.1016/j.molliq.2016.07.048.

[9] M.L. Alcantara, J.P. Santos, M. Loreno, P.I.S. Ferreira, M.L.L. Paredes, L. Cardozo-Filho, A.K. Silva, L.M. Lião, C.A.M. Pires, S. Mattedi, Low viscosity protic ionic liquid for CO2/CH4 separation: Thermophysical and high-pressure phase equilibria for diethylammonium butanoate, Fluid Phase Equilib 459 (2018) 30–43. https://doi.org/https://doi.org/10.1016/j.fluid.2017.12.001.

[10] A. Mota-Lima, M.L. Alcantara, F.J. Pérez-Sanz, R.C. Bazito, P. Vidinha, R.M.B. Alves, C.A. Oller Nascimento, Review - High-Pressure Carbon Dioxide Separation Using Ionic Liquids: A CO2-Electrocatalysis Perspective, J Electrochem Soc 168 (2021) 086502. https://doi.org/10.1149/1945-7111/ac085d.

[11] R. Ratti, Ionic Liquids: Synthesis and Applications in Catalysis, Advances in Chemistry 2014 (2014) 1–16. https://doi.org/10.1155/2014/729842.

[12] W.C. Tu, L. Weigand, M. Hummel, H. Sixta, A. Brandt-Talbot, J.P. Hallett, Characterisation of cellulose pulps isolated from Miscanthus using a low-cost acidic ionic liquid, Cellulose 27 (2020). https://doi.org/10.1007/s10570-020-03073-1.

[13] J. Khan, S. Muhammad, L.A. Shah, J. Ali, M. Ibrar, K.U. Rehman, Synthesis, characterization and electrochemistry of triethyl ammonium sulphate ionic liquid, Zeitschrift Fur Physikalische Chemie 235 (2021). https://doi.org/10.1515/zpch-2020-1704.

[14] N.S.O. Plácido, A.L.S. Carlos, J.U.S. Galvão, R.L. Souza, C.M.F. Soares, S. Mattedi, A.T. Fricks, Á.S. Lima, Protic ionic liquids as a constituent of biphasic systems based on acetonitrile: Phase diagram and alkaloid partitioning, Sep Purif Technol 200 (2018). https://doi.org/10.1016/j.seppur.2018.02.019.

[15] H.M. Choi, I. Kwon, Dissolution of zein using protic ionic liquids: N - (2-hydroxyethyl) ammonium formate and N - (2-hydroxyethyl) ammonium acetate, Ind Eng Chem Res 50 (2011). https://doi.org/10.1021/ie1007745.

[16] Y. Li, J.Y. Dai, Z.L. Xiu, Salting-out extraction of acetoin from fermentation broths using hydroxylammonium ionic liquids as extractants, Sep Purif Technol 240 (2020). https://doi.org/10.1016/j.seppur.2020.116584.

[17] M.L. Alcantara, J.P. Santos, M. Loreno, P.I.S. Ferreira, M.L.L. Paredes, L. Cardozo-Filho, A.K. Silva, L.M. Lião, C.A.M. Pires, S. Mattedi, Low viscosity protic ionic liquid for CO 2 /CH 4 separation: Thermophysical and high-pressure phase equilibria for diethylammonium butanoate, Fluid Phase Equilib 459 (2018) 30–43. https://doi.org/10.1016/j.fluid.2017.12.001.

[18] T.L. Greaves, A. Weerawardena, C. Fong, I. Krodkiewska, C.J. Drummond, Protic Ionic Liquids: Solvents with Tunable Phase Behavior and Physicochemical Properties, J Phys Chem B 110 (2006) 22479–22487. https://doi.org/10.1021/jp0634048.

[19] B.K. Chennuri, R.L. Gardas, Measurement and correlation for the thermophysical properties of hydroxyethyl ammonium based protic ionic liquids: Effect of temperature and alkyl chain length on anion, Fluid Phase Equilib 427 (2016) 282–290. https://doi.org/10.1016/j.fluid.2016.07.022.

[20] N.H.Z.O. Zailani, N.M. Yunus, A.H. Ab Rahim, M.A. Bustam, Experimental Investigation on Thermophysical Properties of Ammonium-Based Protic Ionic Liquids and Their Potential Ability towards CO2 Capture, Molecules 27 (2022) 851. https://doi.org/10.3390/molecules27030851.

[21] R. Turton, R.C. Bailie, W.B. Whiting, J.A. Shaeiwitz, J.A. Shaeiwit, Analysis, Synthesis, and Design of Chemical Processes, (2008).

[22] Progress and Developments in Ionic Liquids, 2017. https://doi.org/10.5772/62621.

[23] M.A. Satyro, Thermodynamics and the Simulation Engineer, Chemical Product and Process Modeling 3 (2008). https://doi.org/10.2202/1934-2659.1077.

[24] T. Altamash, M. Khraisheh, M.F. Qureshi, M.A. Saad, S. Aparicio, M. Atilhan, Cost-effective alkylammonium formate-based protic ionic liquids for methane hydrate inhibition, J Nat Gas Sci Eng 58 (2018) 59–68. https://doi.org/10.1016/J.JNGSE.2018.08.002.

[25] F. Eckert, A. Klamt, Fast solvent screening via quantum chemistry: COSMO-RS approach, AIChE Journal 48 (2002) 369–385. https://doi.org/10.1002/aic.690480220.

[26] A. Klamt, V. Jonas, T. Bürger, J.C.W. Lohrenz, Refinement and parametrization of COSMO-RS, Journal of Physical Chemistry A (1998). https://doi.org/10.1021/jp980017s.

[27] A. Klamt, Conductor-like screening model for real solvents: A new approach to the quantitative calculation of solvation phenomena, Journal of Physical Chemistry (1995). https://doi.org/10.1021/j100007a062.

[28] A. Klamt, The COSMO and COSMO-RS solvation models, Wiley Interdiscip Rev Comput Mol Sci 8 (2018). https://doi.org/10.1002/wcms.1338.

[29] L. Gan, Predicting Density and Viscosity for Liquid Metals and Alloys Using Machine Learning, Int J Thermophys 43 (2022) 99. https://doi.org/10.1007/s10765-022-03035-8.

[30] H. Matsukawa, M. Kitahara, K. Otake, Estimation of pure component parameters of PC-SAFT EoS by an artificial neural network based on a group contribution method, Fluid Phase Equilib 548 (2021) 113179. https://doi.org/10.1016/J.FLUID.2021.113179.

[31] R.K. Cersonsky, B. Cheng, D. Kofke, E.A. Müller, Machine Learning for Generating and Analyzing Thermophysical Data: Where We Are and Where We're Going, J Chem Eng Data 69 (2024) 2041–2043. https://doi.org/10.1021/ACS.JCED.4C00207/ASSET/IMAGES/LARGE/JE4C00207_0001.JPEG.

[32] P. Dehury, S. Chaudhari, T. Banerjee, S. Kumar Das, Prediction of thermophysical properties of deep eutectic solvent-based organic nanofluids: A machine learning approach, J Mol Liq 411 (2024) 125809. https://doi.org/10.1016/J.MOLLIQ.2024.125809.

[33] BIOVIA, REFERENCE MANUAL of COSMOtherm 2021, FRANCE, 2020.

[34] K.I.M. Al-Malah, Aspen Plus®, Wiley, 2016. https://doi.org/10.1002/9781119293644.

[35] Dassault Systèmes., BIOVIA COSMOtherm, (2021).

[36] M.L. Alcantara, G. de Almeida Oliveira, L.M. Lião, C.P. Borges, S. Mattedi, Amine/Carboxylic Acid Ionic Liquid Composite Membranes for CO2 Separation, Ind Eng Chem Res 60 (2021) 4405–4419. https://doi.org/10.1021/acs.iecr.0c06083.

[37] M.L. Alcantara, P.I.S. Ferreira, G.O. Pisoni, A.K. Silva, L. Cardozo-Filho, L.M. Lião, C.A.M. Pires, S. Mattedi, High pressure vapor-liquid equilibria for binary protic ionic liquids + methane or carbon dioxide, Sep Purif Technol 196 (2018) 32–40. https://doi.org/10.1016/j.seppur.2017.08.013.

[38] D. Santos, F. Costa, E. Franceschi, A. Santos, C. Dariva, S. Mattedi, Synthesis and physico-chemical properties of two protic ionic liquids based on stearate anion, Fluid Phase Equilib 376 (2014) 132–140. https://doi.org/10.1016/j.fluid.2014.05.043.

[39] A.C. Belusso, S. Mattedi, R. de P. Soares, P.B. Staudt, Vapor–liquid equilibrium for protic ionic liquids and water: [BA][Pr], [DEA][Pr], [m-2HEA][Pr] and [e-2HEA][Pr], J Chem Thermodyn 182 (2023) 107034. https://doi.org/10.1016/j.jct.2023.107034.

[40] C. Florindo, F.S. Oliveira, L.P.N. Rebelo, A.M. Fernandes, I.M. Marrucho, Insights into the Synthesis and Properties of Deep Eutectic Solvents Based on Cholinium Chloride and Carboxylic Acids, ACS Sustain Chem Eng 2 (2014) 2416–2425. https://doi.org/10.1021/sc500439w.

[41] C. Steffen, K. Thomas, U. Huniar, A. Hellweg, O. Rubner, A. Schroer, TmoleX—A graphical user interface for TURBOMOLE, J Comput Chem 31 (2010) 2967–2970. https://doi.org/10.1002/jcc.21576.

[42] I. Khan, K.A. Kurnia, T.E. Sintra, J.A. Saraiva, S.P. Pinho, J.A.P. Coutinho, Assessing the activity coefficients of water in cholinium-based ionic liquids: Experimental measurements and COSMO-RS modeling, Fluid Phase Equilib 361 (2014) 16–22. https://doi.org/10.1016/j.fluid.2013.10.032.

[43] TURBOMOLE, TURBOMOLE V7.4 2019, a development of University of Karlsruhe and Forschungszentrum Karlsruhe GmbH, 1989-2007, (2019). www.turbomole.com (accessed July 22, 2024).

[44] K. Paduszyński, Extensive Evaluation of the Conductor-like Screening Model for Real Solvents Method in Predicting Liquid-Liquid Equilibria in Ternary Systems of Ionic Liquids with Molecular Compounds, Journal of Physical Chemistry B 122 (2018) 4016–4028. https://doi.org/10.1021/acs.jpcb.7b12115.

[45] S. Grimme, J. Antony, S. Ehrlich, H. Krieg, A consistent and accurate *ab initio* parametrization of density functional dispersion correction (DFT-D) for the 94 elements H-Pu, J Chem Phys 132 (2010). https://doi.org/10.1063/1.3382344.

[46] M. Diedenhofen, A. Klamt, COSMO-RS as a tool for property prediction of IL mixtures—A review, Fluid Phase Equilib 294 (2010) 31–38. https://doi.org/10.1016/j.fluid.2010.02.002.

[47] I.S. O, J.C.F.G.I.M. Jcgm, Evaluation of measurement data — Guide to the expression of uncertainty in measurement, International Organization for Standardization Geneva ISBN 50 (2008) 134. https://doi.org/10.1373/clinchem.2003.030528.

[48] S.L.R. Ellison, M. Rosslein, A. Williams, L.A. Konopel'ko, A. V Garmash, EURACHEM/CITAC Guide: Quantifying Uncertainty in Analytical Measurement, Journal of Analytical Chemistry 58 (2003) 191. https://doi.org/10.1023/A:1022374509064.

[49] L.M. Follegatti–Romero, F.H.B. Sosa, M.C. Costa, D.T. Tavares, L.H. de Oliveira, L.A. Follegatti–Romero, Excess volumes and partial molar volumes of binary liquid mixtures of furfural or 2–methylfuran with alcohols at 298.15 K, J Chem Thermodyn 134 (2019) 20–30. https://doi.org/10.1016/J.JCT.2019.02.027.

[50] K.V.M. Cavalcanti, L.M.L.A. Follegatti-Romero, I. Dalmolin, L.M.L.A. Follegatti-Romero, Liquid-liquid equilibrium for (water + 5-hydroxymethylfurfural + 1-pentanol/1-hexanol/1-heptanol) systems at 298.15 K, J Chem Thermodyn 138 (2019) 59–66. https://doi.org/10.1016/J.JCT.2019.06.010.

[51] C. Schütter, A. Bothe, A. Balducci, Mixtures of acetonitrile and ethyl isopropyl sulfone as electrolytes for electrochemical double layer capacitors, Electrochim Acta 331 (2020) 135421. https://doi.org/10.1016/j.electacta.2019.135421.

[52] A. Drozd-Rzoska, S.J. Rzoska, Consistency of the Vogel — Fulcher — Tammann (VFT) Equations For The Temperature-, Pressure-, Volume-and Density- Related Evolutions of Dynamic Properties in Supercooled and Superpressed Glass Forming Liquids/Systems, in: 2010: pp. 93–106. https://doi.org/10.1007/978-90-481-3408-3_7.

[53] H. Wang, W. Dong, Z. Hou, L. Cheng, X. Li, L. Huang, Direct amidation of non-activated carboxylic acid and amine derivatives catalyzed by $TiCp_2Cl_2$, Appl Organomet Chem 34 (2020). https://doi.org/10.1002/aoc.5568.

[54] B. Pan, D.-M. Huang, H.-T. Sun, S.-N. Song, X.-B. Su, Heterocyclic Boron Acid Catalyzed Dehydrative Amidation of Aliphatic/Aromatic Carboxylic Acids with Amines, J Org Chem 88 (2023) 2832–2840. https://doi.org/10.1021/acs.joc.2c02515.

[55] M.J. Earle, J.M.S.S. Esperança, M.A. Gilea, J.N. Canongia Lopes, L.P.N. Rebelo, J.W. Magee, K.R. Seddon, J.A. Widegren, The distillation and volatility of ionic liquids, Nature 439 (2006) 831–834. https://doi.org/10.1038/nature04451.

[56] M.L. Alcantara, P.H.R. Silva, L.L. Romanielo, L. Cardozo-Filho, S. Mattedi, Effect of water on high-pressure ternary phase equilibria of CO2 + H2O + alkanolamine based ionic liquid, J Mol Liq 306 (2020) 112775. https://doi.org/10.1016/j.molliq.2020.112775.

[57] M.L. Alcantara, M.L. de Carvalho, V.H. Álvarez, P.I.S. Ferreira, M.L.L. Paredes, L. Cardozo-Filho, A.K. Silva, L.M. Lião, C.A.M. Pires, S. Mattedi, High pressure vapor-liquid equilibria for binary carbon dioxide and protic ionic liquid based on ethanolamines + butanoic acid, Fluid Phase Equilib 460 (2018) 162–174. https://doi.org/10.1016/j.fluid.2017.12.018.

[58] V.H. Alvarez, S. Mattedi, M. Aznar, Density, refraction index and vapor-liquid equilibria of N-methyl-2-hydroxyethylammonium butyrate plus (methyl acetate or ethyl acetate or propyl acetate) at several temperatures, Journal of Chemical Thermodynamics 62 (2013) 130–141. https://doi.org/10.1016/j.jct.2013.02.022.

[59] R.R. Pinto, S. Mattedi, M. Aznar, Synthesis and Physical Properties of Three Protic Ionic Liquids with the Ethylammonium Cation, 43 (2015) 1165–1170. https://doi.org/10.3303/CET1543195.

[60] L.M.C. Oliveira, F.R.G. Ribeiro, M.L. Alcantara, G.O. Pisoni, V.F. Cabral, L. Cardozo-Filho, S. Mattedi, High pressure vapor-liquid equilibria for binary methane and protic ionic liquid based on propionate anions, Fluid Phase Equilib 426 (2016) 65–74. https://doi.org/10.1016/j.fluid.2016.03.021.

[61] G.L. Bressan, M.L. Alcantara, L.A. Follegatti-Romero, Density, viscosity, and thermal stability of alkanolamine-based ionic liquids, J Mol Liq 413 (2024) 125918. https://doi.org/10.1016/j.molliq.2024.125918.

[62] M.L. Alcantara, G. de Almeida Ribeiro Oliveira, L.M. Lião, A. Ortiz, S. Mattedi, Highly Selective CO_2 /CH_4 Membranes Based on Ethanolamine Ionic Liquids, Ind Eng Chem Res 63 (2024) 8306–8318. https://doi.org/10.1021/acs.iecr.3c04533.

[63] R.D. Chirico, M. Frenkel, J.W. Magee, V. Diky, C.D. Muzny, A.F. Kazakov, K. Kroenlein, I. Abdulagatov, G.R. Hardin, W.E. Acree, J.F. Brenneke, P.L. Brown, P.T. Cummings, T.W. De Loos, D.G. Friend, A.R.H. Goodwin, L.D. Hansen, W.M. Haynes, N. Koga, A. Mandelis, K.N. Marsh, P.M. Mathias, C. McCabe, J.P. O'Connell, A. Pádua, V. Rives, C. Schick, J.P.M. Trusler, S. Vyazovkin, R.D. Weir, J. Wu, Improvement of quality in publication of experimental thermophysical property data: Challenges, assessment tools, global implementation, and online support, J Chem Eng Data 58 (2013) 2699–2716. https://doi.org/10.1021/je400569s.

5. CRediT authorship contribution statement

Murilo L. Alcantara:Conceptualization, visualization, Methodology, software, Supervision, Writing – original draft, review & editing; **Gabriel L. Bressan**: Investigation, data curation, methodology, Methodology, Writing – original draft. **Paulo V. A. Santos**: data curation, methodology, Methodology, Writing – original draft; **Maria F. V. Nobre**: data curation, methodology, Methodology, Writing – original draft; **João A. P. Coutinho**: Resources, Supervision, Writing – review & editing **Luis A. F. Romero**: Project administration, Resources, Supervision, Writing – review & editing.

COSMO-RS and experimental thermophysical properties of alkylammonium ionic liquids

Highlights

- COSMO-RS provided qualitatively accurate predictions of the thermophysical properties of ILs.
- Applying a correction using room temperature data reduced COSMO-RS ARD to 0.27-13.3%.
- Viscosity dropped ~80x, from 896.1 to 10.75 mPa·s, after hydroxyl removal.
- A higher concentration of hydroxyl groups increases the density.
- TZVP paraetrization proved most accurate; separated ions for hydroxyl ILs, ion-pair for non-hydroxyl.